ELSEVIER

Cognitive Brain Research 12 (2001) 75–88

COGNITIVE BRAIN RESEARCH

www.elsevier.com/locate/bres

Research report

Visual activation of frontal cortex: segregation from occipital activity

Clifford D. Saron[a,b,*], Charles E. Schroeder[a,b], John J. Foxe[a,b,d], Herbert G. Vaughan Jr.[b,c]

[a]*Cognitive Neurophysiology Laboratory, Program in Cognitive Neuroscience & Schizophrenia, Nathan Kline Institute for Psychiatric Research, 140 Old Orangeburg Road, Bldg 35, Orangeburg, NY 10962, USA*

[b]*Department of Neuroscience, Albert Einstein College of Medicine, 1300 Morris Park Avenue, Bronx, NY 10461, USA*

[c]*Department of Neurology, Albert Einstein College of Medicine, 1300 Morris Park Avenue, Bronx, NY 10461, USA*

[d]*Department of Psychiatry and Behavioral Science, Albert Einstein College of Medicine, 1300 Morris Park Avenue, Bronx, NY 10461, USA*

Accepted 13 March 2001

Abstract

Studies in primates have found visually responsive neurons that are distributed beyond cortical areas typically described as directly involved in vision. Among these areas are premotor cortex, supplementary motor area, dorsolateral prefrontal cortex and frontal eye fields. Given these findings, visual stimulation would be expected to result in activation of human frontal cortex. However, few human studies have described sensory activations in frontal regions in response to simple visual stimulation. Such studies have classically described event-related potential (ERP) components over occipital regions. The present study sought to further characterize the spatiotemporal dynamics of visually-evoked electrocortical responses elicited by simple visual stimuli using scalp current density measures derived from high-density ERP recordings, with particular emphasis on the distribution of stimulus-related activity over frontal cortex. Hemiretinal stimuli were viewed passively and during a simple ipsi- or contramanual (RT) task. The motor requirement was included to investigate the effects of response preparation on premovement frontal activations. The results indicate early frontocentral activation, particularly over the right hemisphere (peak magnitude 124–148 ms) that is independent of input visual field or motor response requirement, and that is clearly separate in timecourse from the posterior responses elicited by visual input. These findings are in accord with the multiplicity of visual inputs to frontal cortex and are discussed in terms of frontal lobe functions as may be required in these tasks. © 2001 Elsevier Science B.V. All rights reserved.

Theme: Motor systems and sensorimotor integration

Topic: Cortex

Keywords: Visual activation; Frontal cortex; Occipital activity; Spatial attention; High-density mapping; Event-related potential; Scalp current density

1. Introduction

Numerous single unit studies in primates have found visually responsive neurons that are widely distributed within the cerebral cortex beyond areas that are typically described as directly involved in vision. Among these areas are premotor cortex (PMC) [61,60,10,30,77] supplementary motor area (SMA) [18,64] dorsolateral prefrontal cortex (PFC) [37,27,28] and frontal eye fields (FEF) [66,25].

These physiological findings are well supported by anatomical studies that describe inputs from visual cortex to these regions. Wise et al. [76] summarize pathways from parieto-occipital visual areas (PO, V6A) that project both directly and indirectly to dorsal premotor regions. Extensive connections exist between PMC and SMA that can subserve sensory activation of SMA [46,62]. Visually responsive cells in dorsolateral prefrontal cortex are likely mediated by the extensive network of parietal-frontal pathways described by Cavada and Goldman-Rakic [12] and recently by Petrides and Pandya [56]. Additional visual input to this area includes thalamocortical inputs to prefrontal cortex from the pulvinar, which receives distributed visual input from a variety of sources [5,29]. The FEF receive extensive projections from multiple extrastriate visual areas of both the dorsal and ventral streams [65].

Given these findings from primate studies, visual stimulation would be expected to result in activation of human

*Corresponding author. Tel.: +1-845-398-6547; fax: +1-845-398-6545.

E-mail address: saron@nki.rfmh.org (C.D. Saron).

0926-6410/01/$ – see front matter © 2001 Elsevier Science B.V. All rights reserved.
PII: S0926-6410(01)00036-2

frontal cortex. Several recent human studies have demonstrated frontal activation during perceptual tasks. Culham et al. [17] used fMRI to detect activation (in the absence of saccades) in FEF during attentive tracking (but not passive viewing) of a bouncing ball display. Clarke et al. [13] examined sensory-evoked spike-wave complexes from intracerebral depth recordings in the dorsolateral prefrontal cortex of an epileptic patient. Responses to hemifield visual stimuli were seen by 117 ms, with greater amplitude in the hemisphere contralateral to the stimulus. Recently, Blanke et al. [7] reported robust visual event-related potentials (ERPs) in response to passive viewing of simple hemifield stimuli from contralateral FEF recorded subdurally after identification of FEF by electrical stimulation. Endo et al. [23] demonstrated, using whole-head magnetoencephalography (MEG) in a go/no-go task, visual responses in motor regions during no-go trials as well as during passive viewing control conditions. Also using whole-head MEG, Kawamichi et al. [40] found that equivalent current dipoles localized to premotor cortex after occipital and parietal activations in a hand orientation covert discrimination task.

Despite these findings, few human studies using electrocortical or neuromagnetic measures have described sensory activations in frontal regions in response to simple visual stimulation. Such studies have classically characterized ERP components over occipital regions [8,32,70,48]. Even recent studies using dipole localization methods with multi-channel EEG [53,36], 122-channel whole-head MEG [2,33], or combined fMRI and high-density ERP recordings obtained simultaneously [9] localize activation in response to patterned stimuli (onset or reversal) to occipital cortex.

However, reference to the possibility that ERP recordings from frontal electrodes might reflect sensory-related activations separate from the volume-conducted effects of the major occipital response was made by Hajdukovic et al. in 1984 [31]. Subsequent studies by Kurita-Tashmia et al. [44,45] demonstrated amplitude disassociations between occipital P100 and frontal N100 by modifying shape [44] and contrast ratio [45] of pattern-reversal stimuli based on recordings of eight and two channels, respectively. Using 28 channel recordings, Hughes et al. [35] found latency differences (~4 ms, up to 19 ms) between occipital P100 and frontal N100 in 70% of 125 instances, an observation interpreted as evidence of sensory-evoked frontal activity. Further ERP evidence for a disassociation between occipital and frontal activations comes from a recent study by Thorpe et al. [72]. Visual stimuli were presented in a go/no-go categorical decision reaction time (RT) task that required determination of the presence or absence of animals in photographs of natural scenes. By 150 ms, responses from frontal electrodes differentiated the two stimulus types, while occipital responses did not. This finding was interpreted as reflecting a role of frontal cortex in decision making after analysis of the visual scene in more posterior regions, although contributions of visuomotor activation to the differential frontal response cannot be ruled out on the basis of the go/no-go design.

Two recent reports of frontal cortex activation in response to simple visual stimuli come from studies using multiple stationary dipole source estimation techniques (BESA). Simpson et al. [69] describe anterior cingulate and dorsolateral prefrontal sources with peak latencies ~120 ms obtained from 32 channel recordings during a spatial attention task to hemiretinal stimuli. In a study of attention to color effects, Anllo-Vento et al. [4] performed a BESA analysis on the attended–non-attended difference wave grand average across 16 subjects using 32 channel recordings. The eight-dipole mirror-symmetric solution included two dipoles located in left and right inferior premotor cortex that were interpreted as sensory activation in premotor regions via pathways presented above. Finally, Thut et al. [73] found sensory-related frontal activations in an ERP study using source estimation as well as intracranial recordings during a simple visuomotor task similar to that of the present experiment.

In light of these findings, we sought to further characterize the spatiotemporal dynamics of visually-evoked electrocortical responses elicited by simple visual stimuli using high-density ERP recordings (62 and 124 channels), with particular emphasis on the distribution of stimulus-related activity over frontal cortex. Hemiretinal stimuli were viewed passively and during a simple ipsi- or contramanual RT task. The motor requirement was included to investigate the effects of response preparation on premovement frontal activations.

Scalp current density (SCD), derived from scalp potential, was used as the measure of cortical activity, in addition to traditional potential measures for two reasons: (1) SCD measurements, being estimates of the second spatial derivative of potential (or 'Laplacian'), are mathematically reference-independent, unlike potential recordings, which are differences between two recording electrodes; and (2) of particular importance for physiological interpretation, the Laplacian operation that estimates SCD eliminates the potential changes at the scalp due to the passive lateral spread of currents within the scalp itself. This produces a quantity that is directly proportional to transcranial current flow, as well as sharpening the estimates of the active cortical regions by producing clear current density foci [54,74]. Since scalp-recorded potential differences and the transcranial currents estimated by SCD both represent volume conducted currents that are initiated at the sites of transmembrane current flows associated with neural activity within the brain, local SCD magnitude and timing provide measures of the activation of underlying intracortical neural ensembles.

Large interindividual differences have been found in anatomic [11,71,51,41] and functional [1,21,34] brain organization. As such, the approach taken here presents individual subject data. The results indicate, for all sub-

jects, early frontocentral activation, particularly over the right hemisphere (peak magnitude 124–148 ms) that is independent of input visual field or motor response requirement, and that is clearly separate in timecourse from the posterior responses elicited by visual input. These findings are in accord with the multiplicity of visual inputs to frontal cortex as described above.

2. Materials and methods

2.1. Subjects

Three right-handed males between 25 and 33 years of age were tested. All subjects provided written informed consent, and the procedures were approved by the Institutional Review Board of the Albert Einstein College of Medicine where the experiments were conducted. Subjects were compensated $10.00/h. Right-handedness was determined by scoring 9 or higher on the Edinburgh inventory of handedness [52]. Visual acuity was assessed and corrected to 20/40 or better for each eye. All subjects were experienced in this type of physiological recording and task situation.

2.2. Stimuli

Stimuli were presented using Neuroscan Corp. (www.neuro.com) GENTASK software. Stimuli were obliquely oriented parafoveal checkerboard sectors (2° from fixation, 3° in extent) presented in the left or right lower quadrants of the visual fields. Stimuli were generated by single computer screen refreshes and were 6.8 ms in duration. Subjects were seated in a darkened black room 107 cm from a masked 21″ NEC 6FG computer monitor. The intensity of the white checks was 85 cd/m^2 measured at the screen. Stimuli were presented on a dark gray background (contrast ratio 16:1). A central fixation point consisting of a white plus sign (subtending 0.14°) was visible throughout each block of trials.

2.3. Procedure

Left visual field (LVF) or right visual field (RVF) stimuli were briefly presented in two task situations while subjects maintained central fixation: (1) passive viewing; and (2) performance of a simple unimanual (index finger lift) RT task. There were four conditions in the RT task: (1) LVF input/left hand (LH) response; (2) LVF input/right hand (RH) response; (3) RVF/LH; and (4) RVF/RH. In addition, blocks of self-initiated left or right finger lifts were performed interleaved with these six conditions. Data from these trials are not included in the present analysis. Stimulus presentation and response requirements were blocked by condition. Each block consisted of 63 trials for Subjects 1 and 2 and 50 trials for Subject 3. Fixation compliance was video monitored during practice trails and via lateral EOG during data collection. The inter-stimulus interval (ISI) randomly varied from 1.0 to 4.0 s for Subjects 1 and 2 and 1.5 to 3.5 s for Subject 3. Twelve blocks of the passively viewed stimuli and 24 blocks for each of the four RT conditions were presented during three testing sessions (given on consecutive days) for Subjects 1 and 2, and two consecutive days for Subject 3. This yielded 756 trials per passive view condition and 1512 trials per RT condition for Subjects 1 and 2, and 600 trials per passive view condition and 1200 trials per RT condition for Subject 3. For all subjects, condition order was counterbalanced, and counterbalance order was randomized across days and subjects.

2.4. Reaction time recording

Subjects placed the index finger of the appropriate hand on a custom optical switch located at body midline on a table in front of them. Subjects were instructed to lift their index finger off the switch as quickly as possible after each stimulus. Photocell excitation was provided by two small masked flashlights on either side of the optical switch.

2.5. EEG recording

EEG was recorded with 62 scalp sites from Subjects 1 and 2, and 124 scalp sites from Subject 3. Two custom electrode caps (ElectroCap International) were used. The electrode locations are shown in Fig. 1B. The electrode arrays were designed to uniformly sample the upper head in a roughly hemispherical fashion. All subjects had their heads shaved just prior to their first experimental session. All electrode sites were treated with Omniprep and then Electrogel electrolyte. A reference electrode was placed at the tip of the nose. The EEG was amplified using two or four Neuroscan Synamp 32-channel DC amplifier systems. Electrode impedance was maintained below 10 kΩ. EEG signals were filtered (DC to 100 Hz bandpass, −12 dB/octave) and continuously digitized at 1 kHz for the duration of each block of trials. Event markers stored with the digitized data indicated stimulus and response onsets for off-line analysis.

2.6. Electrode location measurements

Electrode locations for subsequent optimized spherical fitting were obtained using 3D digitization procedures. For Subjects 1 and 2, a sonic digitizer (Science Accessories) and bite bar were used. The electrode locations for each subject were averaged across all three days to create a master electrode location file. Electrode locations for Subject 3 were obtained using an electromagnetic 3D digitizer (Polhemus Corp).

A set of fiduciary markers to aid in accurate alignment of digitized electrode locations with a fitted sphere for

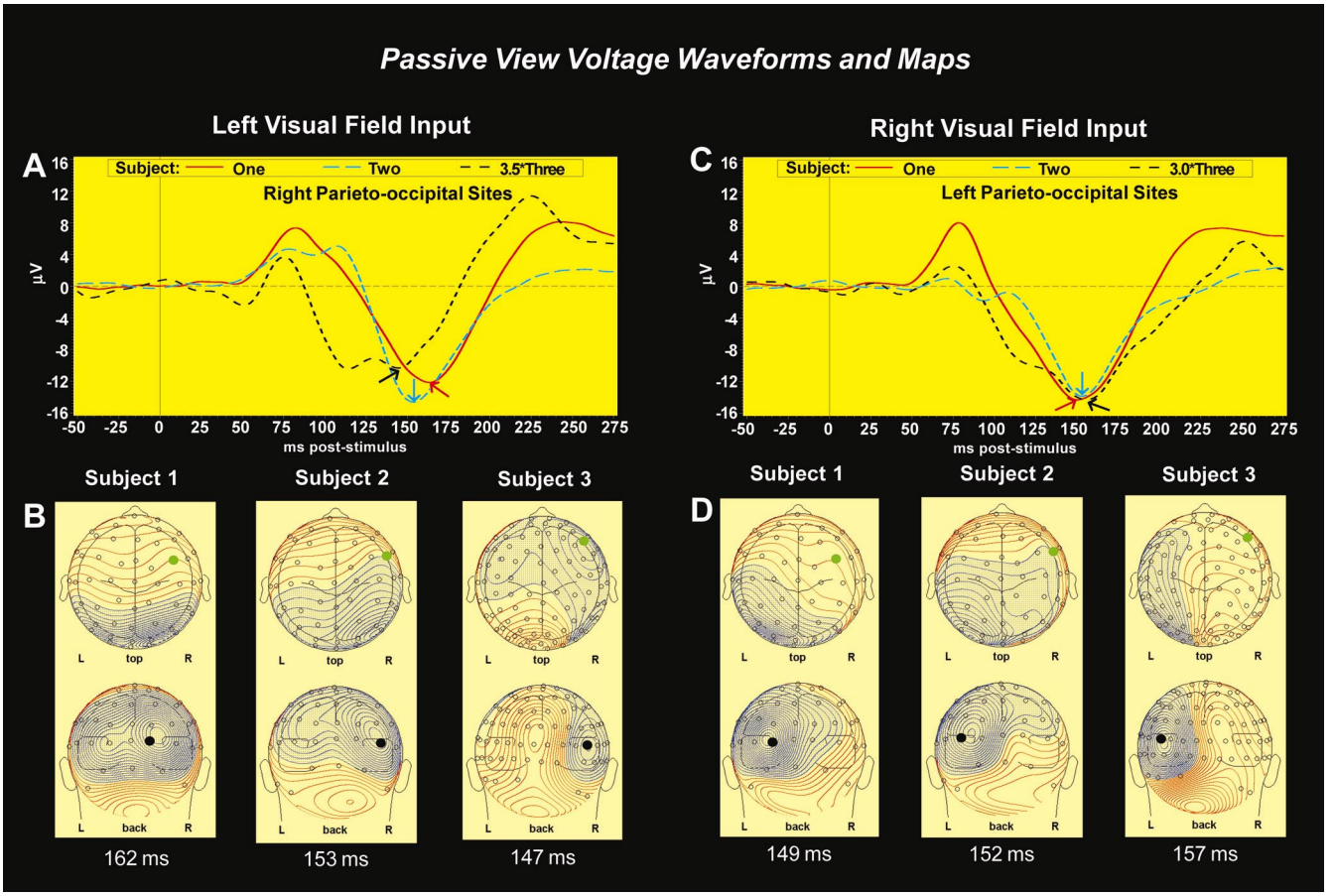

Fig. 1. Voltage ERP waveforms from contralateral parieto-occipital sites and voltage topographic maps elicited by passive viewing of LVF or RVF stimuli are shown for each subject. (A) LVF input. Arrows indicate peak latencies for each subject depicted in the voltage maps of panel (B). Waveforms are referenced to the nose as originally recorded. Values for Subject 3 were multiplied by a factor of 3.5 for display. (B) Top- and back-view spherically interpolated average-reference voltage maps corresponding to the peak latencies shown in panel (A). Locations of recording electrodes are shown by open circles. Electrode locations of waveforms shown in panel (A) are indicated by the filled black circles in the back-view maps. These electrode locations correspond to O2, P6, and PO8 for Subjects 1–3, respectively. Filled green circles in top-view maps correspond to electrode locations of LVF waveforms shown in Fig. 4. Map sensitivity is 0.5, 0.7, and 0.3 μV/line for Subjects 1–3. (C) RVF input. Waveforms as in (A). Values for Subject 3 were multiplied by a factor of 3.0. Electrode locations (indicated by the filled black circles in the back-view of Fig. 1D) correspond to O1, PO5, and PO7 for Subjects 1–3, respectively. Numbers of trials for Subjects 1–3 are: 740, 455, and 567. (D) Average referenced scalp voltage maps for each subject at the peak latencies indicated by the arrows in panel (C). Same sensitivity as in panel (B). See text for further data description.

topographic mapping were placed on each subject at the end of each experimental session. These were located using a Lucite halo as described in Simpson et al. [68]. Polar coordinates of electrode locations fit to this sphere were necessary for subsequent ERP data visualization. For Subjects 1 and 2 these polar coordinates were derived from the *X*, *Y*, and *Z* electrode positions using BESA software (www.megis.com). Polar coordinates for Subject 3 were derived using HADNFD, custom software developed in our laboratory for this purpose by J. Hrabe.

2.7. Data processing and ERP calculation

The continuous data were visually examined, and any trials that lacked a manual response trigger or that contained spurious response triggers were eliminated (usually less than 2% of trials). The data were then epoched for averaging time-locked to stimuli. For Subjects 1 and 3, ERP epochs were −200 to +600 ms pre- and post-stimulus. The epoched data were baseline corrected by subtracting the mean voltage over the interval of −150 to +20 ms. All EEG channels were automatically scanned for artifact with an amplitude threshold of ±75 μV. Above-threshold trials were eliminated from further analysis (typically 10%). Due to EKG artifact in the EEG, data from Subject 2 were treated as follows: ERP epochs were shortened to −100 to +275 ms to minimize rejection of trials based on R spike activity. Epoched data were then baseline corrected using the interval −100 to +20 ms. The artifact threshold for this subject was reduced to ±45 μV to ensure that R spikes within the epoch would be detected. After the automatic artifact rejection, each trial was examined to determine if it was spuriously labeled as artifact, and to ensure that no below-threshold R spikes

went undetected. This overall process resulted in a net loss of 50% of trials. Separate sets of ERPs for each of the six experimental conditions were obtained from all artifact-free trials for each subject, with the constraint that RT be between 120 and 600 ms for all manual response conditions.

2.8. ERP topographic mapping

For each of these six ERPs, the scalp surface potential was spherically interpolated using the polar coordinates of electrode locations and spherical splines according to the method of Perrin et al. [55] as implemented in EEGFOCUS V2.0 software (www.megis.com). The spline smoothing coefficient λ was 1×10^{-7} for Subjects 1 and 2 (62 channel data) and 1×10^{-6} for Subject 3 (124 channel data), values recommended from simulation studies by Babiloni et al. [6]. Prior to interpolation, all ERPs were digitally low-pass filtered at 35 Hz (12 dB/octave, zero phase shift) using EEGFOCUS. The interpolated scalp potentials were then transformed into scalp current density maps (SCD), also using EEGFOCUS.

2.9. Laplacian waveform derivation

For each subject and condition, virtual electrodes ('virtrodes') were placed at the spherical coordinates of the centers of two consistently obtained electrocortical negativities as seen at their peak amplitude within the range of 120 to 170 ms: (1) over the parieto-occipital region of the hemisphere contralateral to the stimulated visual field; and (2) over right frontocentral cortex. Laplacian waveforms at each location were then derived from the spherical spline interpolated SCD data for each condition using EEGFOCUS.

3. Results

3.1. Passive view voltage waveforms and maps

3.1.1. LVF input

Voltage waveforms (as recorded referenced to the nose) from right parieto-occipital sites in response to passive viewing of LVF stimuli are shown for each subject in Fig. 1A. Values for Subject 3 were multiplied by a factor of 3.5 for display. Electrode locations are indicated by the filled black circles in the back-view scalp potential maps of Fig. 1B. These scalp locations correspond to O2, P6, and PO8 sites for Subjects 1–3, respectively, based on the spherical coordinates of the electrodes and the position database in EEGFOCUS. These scalp locations were chosen to coincide most closely with the centers of right posterior scalp potential maxima as shown in Fig. 1B. The numbers of trials for Subjects 1–3 are: 733, 416, and 579. The waveforms for all subjects show an initial positivity (P1) followed by a larger negativity (N1) and a later, more variable positivity. Subject 2 shows a biphasic P1 and Subject 3 shows a biphasic N1, with an earlier onset limb than for other subjects. The arrows indicate the peak latencies that correspond to the scalp potential maps in Fig. 1B.

The spherical spline-interpolated topographic maps of Fig. 1B show the average-referenced scalp potential, along with the positions of the scalp electrodes. The green filled circles on the top-view map correspond to the electrode locations plotted in Fig. 4. Blue corresponds to negative, and red to positive scalp potential. As expected for LVF input, the back-view maps show, for each subject, a right posterior maximum at the N1 peak. The leftward spreading posterior negativity seen for Subjects 1 and 2 also suggests left posterior activation at this time. The top-view maps show a pattern of diffuse central and frontal positivity for Subject 1. The pattern for Subject 2 resembles that of Subject 1, with the addition of a more anterior extent of the broad negativity, particularly over the right hemisphere. The response pattern for Subject 3 differs from Subjects 1 and 2, in that there is a distinct right frontal negativity and indication of a left frontal negativity.

3.1.2. RVF input

Fig. 1C shows nose-referenced voltage waveforms from left parieto-occipital sites in response to passive viewing of RVF stimuli. In contrast the LVF waveforms, Subject 2 does not show a P1 response. However, from ~135 to 175 ms all subjects show a very similar N1 timecourse. The arrows point to the peak latencies that correspond to the Fig. 1D scalp potential maps. The back-view maps of Fig. 1D show the expected left posterior maxima give RVF input. There is less suggestion of bilateral posterior activation at the displayed latencies than seen in Fig. 1B. The top-view maps show left anterior spread of the posterior negativity for all subjects, extending in a broad right frontocentral pattern for Subject 2.

3.2. Passive view laplacian waveforms and SCD maps

3.2.1. LVF input

Laplacian waveforms and SCD maps from the LVF passive view condition are presented in Fig. 2. Panel A shows Laplacian waveforms from right parieto-occipital locations that correspond to the centers of inward scalp current shown in the SCD maps of panel B. (Blue corresponds to inward, and red to outward, scalp current, derived from scalp potential). Electrode labels for these virtual electrodes ('virtrodes') are PO4, PO6, and PO8 for Subjects 1–3. Two features of the Panel A waveforms are noteworthy compared to the voltage waveforms of Fig. 1A: (1) the similarity of onset timing of the initial positivity across subjects; and (2) the overall similarity of the inward current N1 corresponding to the scalp potential negativity across subjects. The arrows indicate the timing

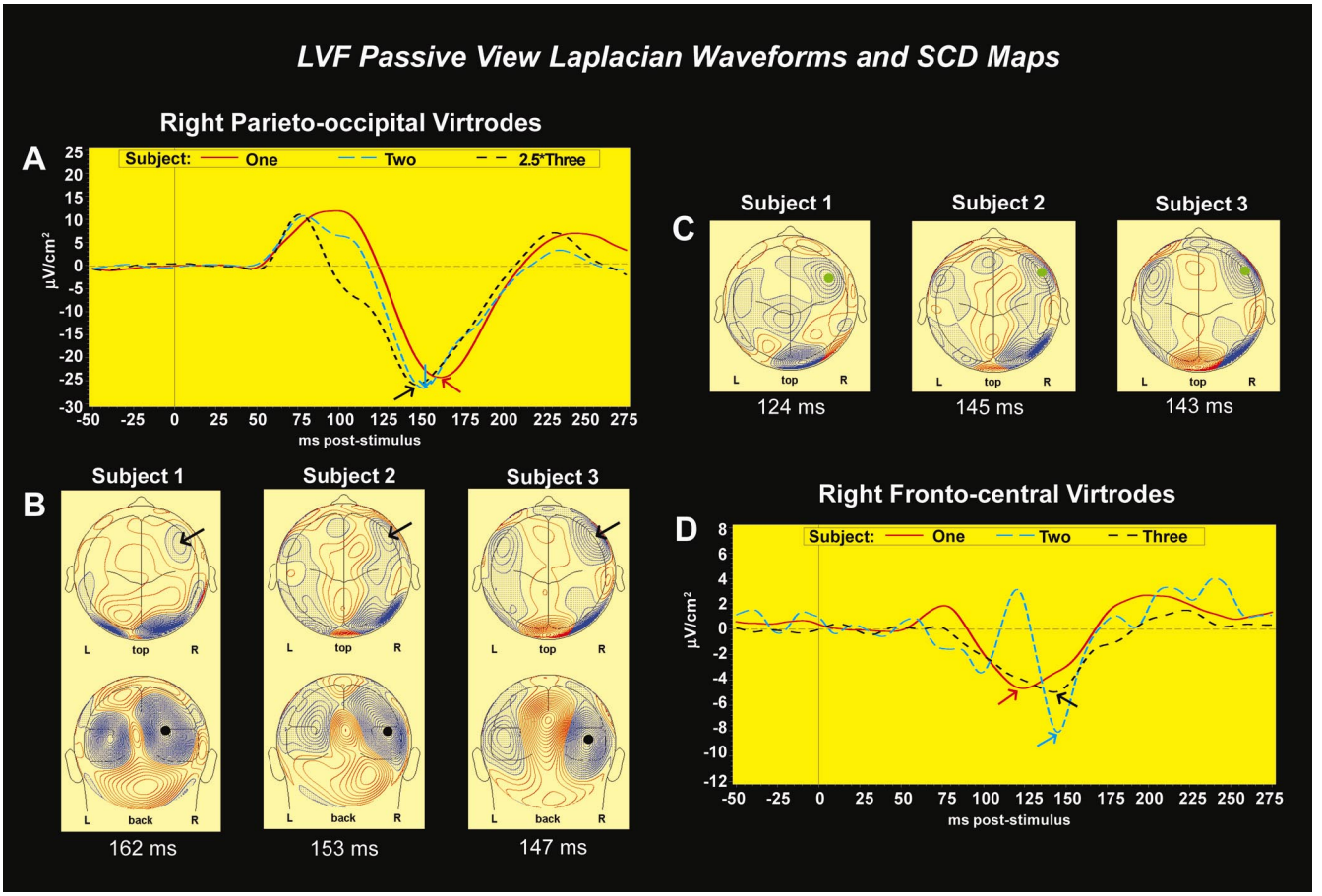

Fig. 2. Laplacian waveforms and SCD maps from the LVF passive view condition. (A) Laplacian waveforms from right parieto-occipital locations that correspond to the centers of inward scalp current shown as black filled circles in the back view SCD maps of panel (B). (B). Top- and back-view SCD maps corresponding to the peak latencies indicated by the arrows in panel (A). These latencies are identical to scalp potential maps of Fig. 1B. Electrode labels for these virtual electrodes ('virtrodes') are PO4, PO6, and PO8 for Subjects 1–3. Blue corresponds to inward, and red to outward, scalp current, derived from scalp potential. Plotted sensitivity is 0.5, 0.7, and 0.3 $\mu V/cm^2$ for Subjects 1–3. The top-view SCD maps show, for each subject, evidence of a right frontocentral negativity (arrows), an activity pattern only suggested by the scalp potential data in Fig. 1B for Subject 3. (C). Top view SCD maps corresponding to the peak latencies indicated by the arrows of panel (D) showing the intersubject consistency of right frontocentral activation. Green filled circles indicate the locations of frontocentral virtrodes shown in panel (D). These locations correspond to FC2, FC6, and FC6 for Subjects 1–3, respectively. (D). Laplacian virtrode waveforms corresponding to right frontocentral foci depicted in panel (C). Two features of these waveforms suggest that the right frontocentral and right parieto-occipital responses represent activation of separate brain regions: (1) peak latencies for the frontocentral N1 precede the posterior response for each subject; and (2) the overall timecourse of the responses differ between regions. Although the right frontocentral activation pattern at N1 peak latency is similar across subjects, the intersubject variability of the frontocentral waveforms stands in contrast to the parieto-occipital Laplacian waveforms, which are globally similar across subjects.

of the SCD maps plotted in Fig. 2B. These latencies are identical to scalp potential maps of Fig. 1B.

In contrast to the Fig. 1B maps, the back-view SCD maps show distinct patterns of bilateral activation for all subjects. The midline posterior positivities seen most prominently for Subjects 2 and 3 likely reflect contributions from both hemispheres due to non-radial source configurations associated with the bilateral negativities. The top-view SCD maps show, for each subject, evidence of a right frontocentral negativity (arrows), an activity pattern only suggested by the scalp potential data in Fig. 1B for Subject 3. The intersubject consistency of this response is indicated by the clear right frontocentral foci visible in the SCD maps of Panel C. The displayed latencies correspond to the peak negativities (at arrows) shown in the frontocentral virtrode waveforms of Panel D, which were derived from the locations indicated by green filled circles in the Panel C SCD maps. The virtrode locations correspond to FC2, FC6, and FC6 for Subjects 1–3, respectively. In addition to the right frontocentral negativities, each subject shows some evidence of bilateral frontocentral activity, as well as midline (Subject 1) and more lateral central activations (Subject 2). Two features of the Laplacian waveforms shown in Panel D suggest that the right frontocentral and right parieto-occipital responses represent activation of separate brain regions: (1) peak latencies for the frontocentral N1 precede the posterior response for each subject; and (2) the overall timecourse of

the responses differ between regions. Although the right frontocentral activation pattern at N1 peak latency is similar across subjects, the intersubject variability of the frontocentral waveforms stands in contrast to the parieto-occipital Laplacian waveforms, which is globally similar across subjects.

3.2.2. RVF input

Laplacian waveforms and SCD maps from the RVF passive view condition are presented in Fig. 3. Panel A shows Laplacian waveforms from left parieto-occipital virtrode locations as indicated by the black filled circles on the back-view SCD maps of panel B. Electrode labels for these virtrodes are O1, O1, and PO7 for Subjects 1–3, respectively. As seen in the results from LVF input, from 50 to 175 ms, the Laplacian waveforms are more similar between subjects than are the voltage counterparts from Fig. 1C, particularly for the P1 component. The average N1 peak latency for RVF input did not differ from LVF input (154 versus 153 ms), suggesting a general equivalence in activation timing for the hemisphere contralateral to visual input. The SCD maps plotted in Fig. 3B correspond to the arrows at the N1 peak, and are from identical times as the scalp potential maps of Fig. 1D.

The back-view SCD maps in Panel 3B show distinct patterns of bilateral activation for all subjects, compared to the broad posterior activation patterns of Fig. 1D. These right posterior foci appear weaker than the left posterior foci observed for LVF input (Fig. 2B). The top-view SCD maps of Panel 3B show, for each subject, bilateral central or frontocentral negativities, including clear right frontocentral foci (arrows), an activity pattern absent in the scalp potential data in Fig. 1D. As was seen in response to LVF input, the consistency of right frontocentral activation across subjects is demonstrated by the SCD maps of Panel C. The displayed latencies correspond to the peak negativities (arrows) shown in the frontocentral virtrode waveforms of Panel D, which were derived from the locations indicated by green filled circles in the Panel C SCD maps. As before, the virtrode locations correspond to FC2, FC6, and FC6 for Subjects 1–3, respectively. In addition to the right frontocentral negativities, each subject

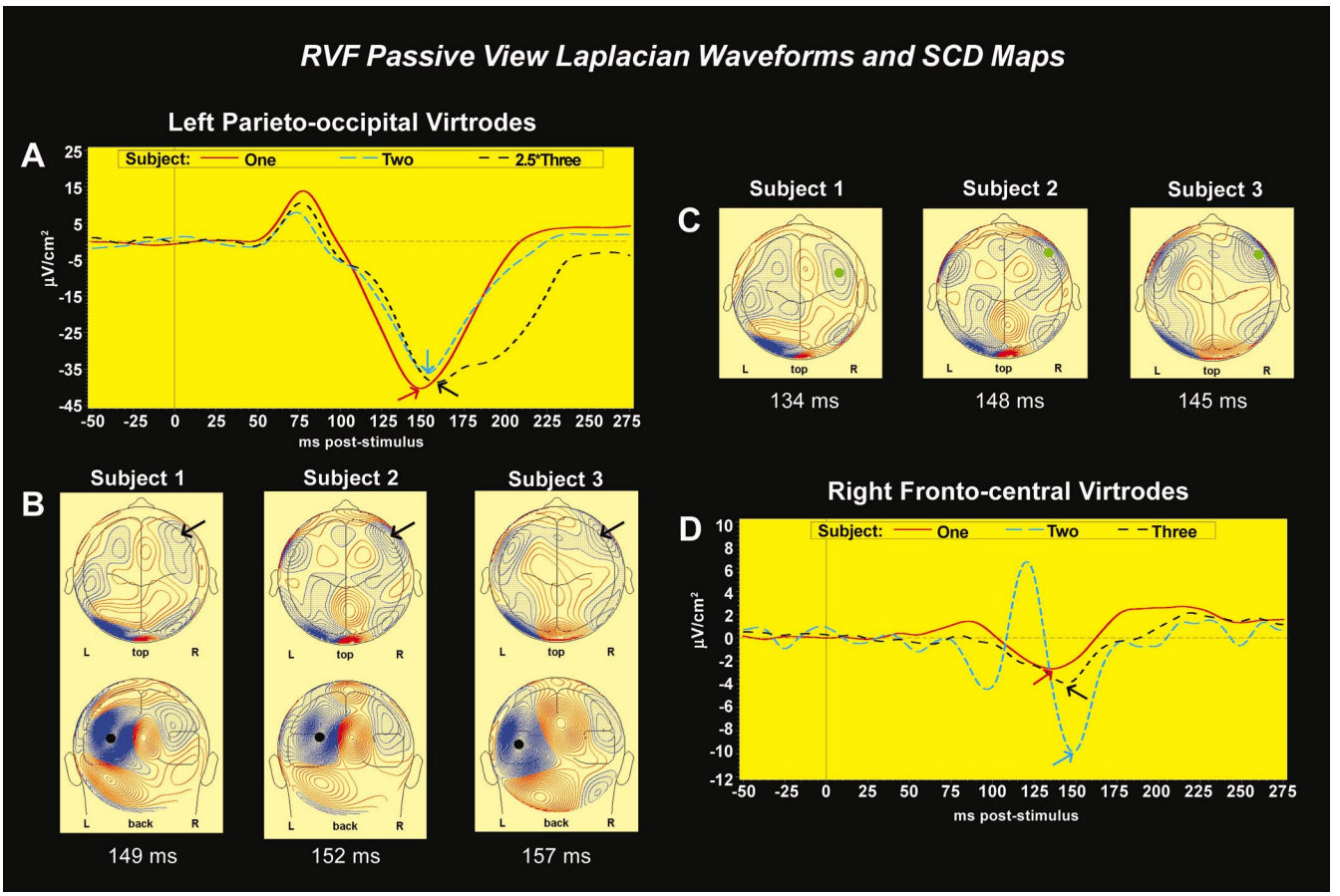

Fig. 3. Laplacian waveforms and SCD maps from the RVF passive view condition. Same format as Fig. 2. (A) Left posterior virtrode waveforms correspond to scalp locations at O1, O1, and PO7 for Subjects 1–3, respectively. (B) Top- and back-view SCD maps at peak latencies of arrows in panel (A) (identical latencies as in Fig. 1D). Arrows indicate frontocentral activations only suggested for Subject 2 in the voltage maps of Fig. 1D. (C) Top-view SCD maps at peak latencies indicated by the arrows in panel (D). Green filled circles correspond to virtrode locations shown in panel (D). (D) Right frontocentral virtrode waveforms (equivalent scalp locations FC2, FC6, and FC6 for Subjects 1–3) as indicated in panel (C). See text for data description.

shows bilateral frontocentral activity. Left hemisphere central and frontocentral activity is more clearly defined for RVF compared with LVF input (Fig. 2C), consistent with the major visual input to left posterior regions with RVF stimulation.

However, there is a striking similarity of the frontocentral Laplacian waveforms shown in Figs. 2D and 3D. The relative independence of right frontocentral activity from input visual field, and earlier N1 peak latencies than seen for the left posterior responses further support the suggestion of separately observable posterior and frontocentral sources of stimulus-related activity.

3.3. Passive view right frontocentral voltage waveforms

Fig. 4 presents voltage waveforms referenced to the nose for right frontocentral electrodes closest to the frontocentral virtrode locations. These recording sites are indicated by the green filled circles in the top-view maps of Fig. 1B and D. The LVF voltage waveforms show, for each subject, longer duration activations than suggested by the corresponding CSD waveforms of Fig. 2D. N1 peak latency timing also differs between voltage and CSD waveforms. For example, N1 voltage peak latency for Subject 3 is 117 ms, compared with 143 ms for the CSD waveform. The earlier voltage peak can be accounted for by volume conduction of the posterior negative peak visible at 117 ms in the Subject 3 waveform of Fig. 1A. Although the N1 peak latency of voltage and CSD waveforms for Subject 2 do not differ, the initial negativity visible at 98 ms in the CSD waveforms is wholly absent in the voltage waveform. The RVF voltage waveforms show similar effects to those seen for the LVF waveforms.

3.4. Passive view versus RT task SCD maps

Top-view SCD maps corresponding to the N1 peak latency of right frontocentral virtrodes from passive view conditions (Figs. 2C and 3C) were compared to equivalent SCD maps obtained from each RT condition. These data are presented in Fig. 5.

The striking feature of this figure is the consistency of the right frontocentral negativity (indicated by arrow) across conditions, independent of the requirements for motor output. Peak amplitude latency values (indicated below the maps) generally differ little between conditions within a visual field. The largest within-field latency deviation is the 12 ms increase for the RVF/RH condition of Subject 1. A second noteworthy aspect of these data is the relative overall similarity, within a visual field and subject, of the bilateral central and frontocentral activation patterns. An exception to this observation is the LVF/LH vs. LVF/RH data from Subject 2 which show a greater magnitude central negativity over the hemisphere contralateral to the response hand. Overall, the independence of the right frontocentral negativity from motor requirements suggests that this activation represents visual activation of frontal cortex.

4. Discussion

The principal finding from this study was that hemiretinal stimuli activated frontal cortex independent of input visual field and motor response requirements. Passive viewing of LVF or RVF input, as well as performance of a simple RT task using left or right hand index finger lifts, consistently resulted in activation of right frontal cortex,

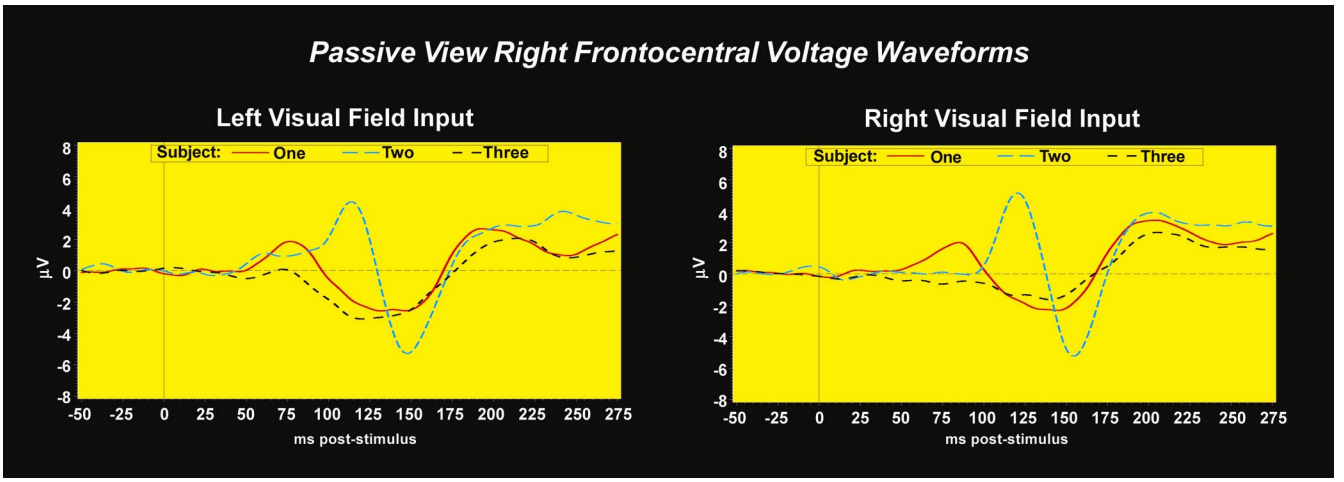

Fig. 4. Right frontocentral nose-referenced voltage waveforms corresponding to scalp locations indicated by green filled circles in the top-view voltage maps Fig. 1B and D for LVF and RVF input, respectively. Note the broader negative peaks for Subjects 1 and 3, and different waveform component structure for Subject 2 compared with the virtrode waveforms of Figs. 2D and 3D.

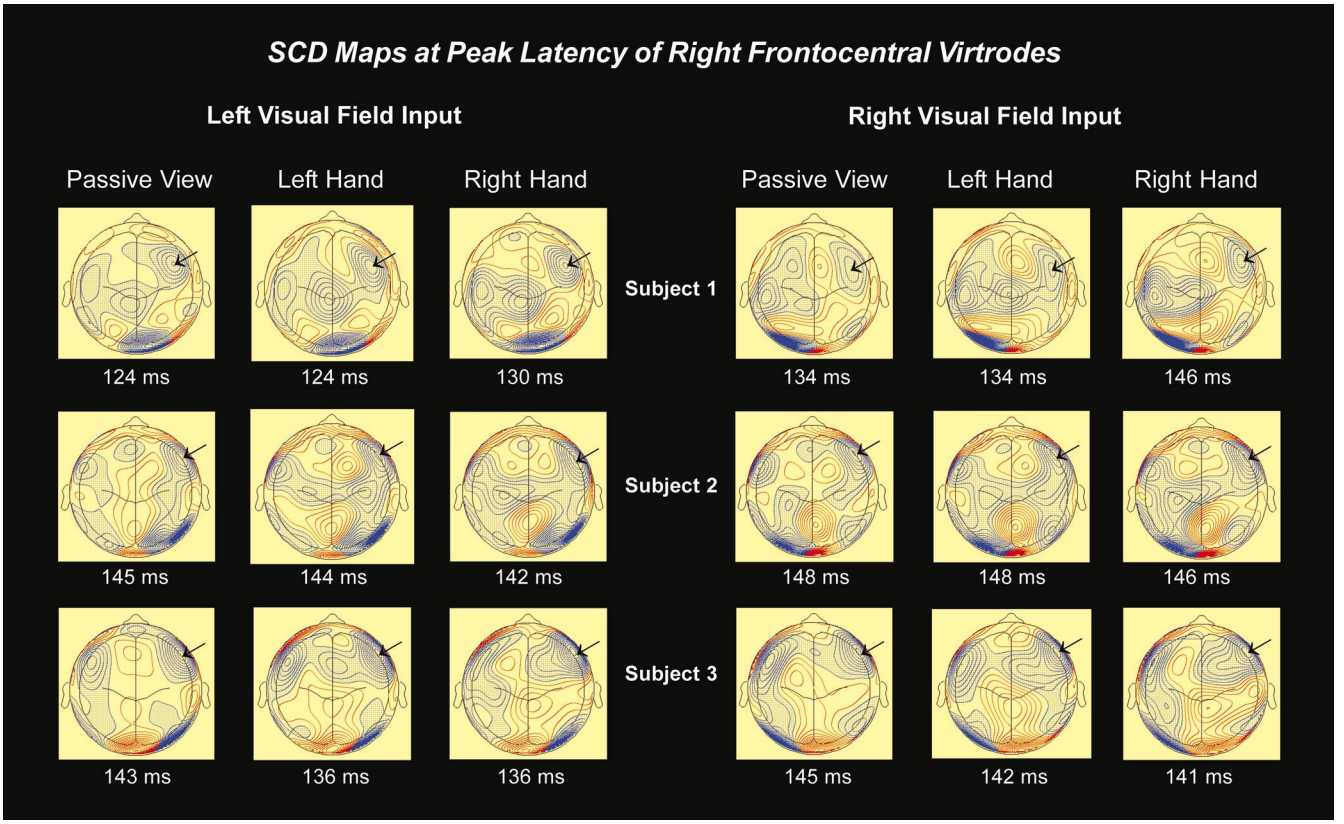

Fig. 5. Top-view SCD maps corresponding to the N1 peak latency of right frontocentral virtrodes from passive view conditions (Figs. 2C and 3C) and the equivalent SCD maps obtained from each RT condition. The numbers of trials for the RT condition are (in order of Subjects 1–3): LVF/LH=1323, 737, and 1093; LVF/RH=1388, 611, and 1113; RVF/LH=1362, 655, and 1163; and RVF/RH=1308, 585, and 1057. Mean median RT across conditions for Subjects 1–3 were: 273, 268 and 316 ms. SCD map latencies (indicated below the maps) correspond to peak amplitude latency values of right frontocentral virtrode waveforms. The striking feature of this figure is the consistency of the right frontocentral negativity (indicated by arrows) across conditions, independent of the requirements for motor output. The independence of the right frontocentral negativity from motor requirements suggests that this activation represents sensory-related activation of frontal cortex.

with peak negativities from 124 to 148 ms. SCD mapping at these latencies also revealed patterns of bilateral frontal activation, in addition to medial and lateral left central activity. These latter observations, particularly central activation patterns, were more dependent on input visual field and task condition. Taken together, the data are consistent with results from primate and human studies that demonstrate visual input-related activations in frontal cortex as reviewed in the introduction.

The data from passive view conditions were presented as both scalp potential and current density. Topographic mapping of SCD measures derived from scalp potential provided clearer visualization of activation foci than was obtained from mapping of average-referenced scalp potential. Further, voltage versus SCD waveforms were more susceptible to the volume-conducted effects of the large posterior negativity elicited from the hemisphere contralateral to visual input, in that frontal waveform component shape and peak latencies of the voltage waveforms were shifted to reflect the timing of posterior activations. The timecourse of frontal SCD measures was more independent of posterior activity. These observations demonstrate the importance of SCD measures, obtained on the basis of large spatial sampling, in depicting the activation timecourse and putative location of electrocortical responses elicited by hemiretinal stimuli. Two central questions frame the main finding of consistent right frontal activation, within the broader context of possible functional roles for frontal activation in the present task conditions: (1) what are the candidate cortical regions underlying this activity? and (2) what additional evidence is there in support of the observed asymmetry of right versus left frontal activity?

4.1. Candidate frontal cortical regions

The location of the right frontal and frontocentral negativity depicted in Fig. 5 is consistent with contributions from multiple regions of frontal cortex. These include PFC, FEF, and PMC. The recent observation of robust

visual ERPs recorded subdurally over human FEF by Blanke et al. [7] in response to hemiretinal input, and the location of FEF by electrical stimulation [7], transcortical magnetic stimulation [63] and fMRI [47,42] support an FEF contribution to the observed right frontal activity, particularly for Subject 1. However, it is important to note that Blanke et al. [7] found clear and consistent large response attenuation when stimuli were presented ipsilateral to the recording sites. This was not the case in the present data, since ipsilateral responses were clearly obtained, with similar amplitude and timing as contralateral responses for Subjects 2 and 3. Subject 1 does, however, show a delayed (mean=12 ms) and diminished right frontocentral response for RVF compared to LVF input, possibly reflecting interhemispheric transfer of the strong left central negativities visible across response conditions for this subject in Fig. 5. The more caudal location of these responses, and the asymmetry for ipsilateral versus contralateral visual input are consistent with a contribution of FEF to responses seen for Subject 1. The location of the right frontal activation for Subjects 2 and 3 appears most likely as reflecting contributions of right dorsolateral prefrontal cortex. The lack of LVF versus RVF difference for these subjects is also closer to the results of Clarke et al. [13], who found left PFC intracortical spike and wave complexes in an epileptic patient in 51% of RVF presentations and 32% of LVF presentations. Activation of PFC has also recently been demonstrated in a visual detection simple RT task using fMRI [20].

4.2. Asymmetrical frontal activation

One way to approach the observation of consistent right frontal activation independent of input visual field or response requirement is to view the task situation in terms of demands of spatial attention, and consider evidence for hemispheric specialization regarding the allocation of spatial attention. Frontal negativities specifically related to spatial attention have been obtained in the latency range of the present data [38] and it is of note that a recent neuroimaging study investigating spatial attention [42] describes a pattern of cortical activation markedly consistent with the present electrophysiological results, as will be described below.

While the ‘passive view’ condition made no demand for an overt response, nor contained an explicit instruction for the allocation of attention, the task situation engaged two features of spatial attention: (1) voluntary maintenance of central fixation during blocked unilateral input; and (2) transitory spatial priming effects due to the occurrence of each stimulus. Activation of prefrontal cortex has been directly associated with the central fixation using PET [3]. Attentional capture by rapid onset peripheral visual stimulation has been demonstrated in a number studies (reviewed in Ref. [22]) and activation of frontal cortex using PET and fMRI has been demonstrated in no-overt-response conditions requiring covert allocation of spatial attention during central fixation and peripheral visual input [14,15]. Thus, to the extent that the transient hemifield input during the passive view condition repeatedly resulted in covert orienting to the stimulated location, regional brain activations associated with covert orienting would be expected to be observed during these conditions, in addition to the sensory responses elicited by the stimuli and prefrontal activation due to central fixation. Further, just the expectation of stimulation at a hemifield location during central fixation has recently been demonstrated to result in bilateral frontal activation using fMRI [39].

Although sustained motor readiness is required during the RT task, the passive-view and RT conditions require essentially the same demands in terms of allocation of spatial attention or elicitation of covert orienting. Therefore to the extent that the observed frontal activations are related to these processes, they would not be expected to differ between passive view and motor output conditions. Behavioral and electrophysiological evidence for effects of covert orienting of spatial attention in a task situation similar to the RT conditions comes from a recent study by Mangun and Buck [49]. Using a mixed, rather than blocked design of the present RT task, this study required directed attention during performance of the task. The three attention conditions were: attend to the LVF, divide attention between the visual fields, and attend to the RVF, while stimuli were presented randomly to the left or right of central fixation shortly after a warning tone. Two features of this study are important for ERP studies of spatial attention. The first is the sustained nature of the attentional instruction over a block of trials (1.5 min) rather than cued for each trial. This makes the experimental manipulation of attention closer to the duration of the sustained attentional requirements of the present task. The second feature is the requirement for a manual response (simple RT) to each stimulus, including non-attended locations. This allows examination of the reaction time costs, as well as benefits, of allocating spatial attention and served as a motor control for attended and unattended locations. Relative to the divided-attention condition, there was, on average, a 12-ms RT benefit for attending to the location of stimuli, and a 35-ms cost for responses made to the unattended stimuli. The direction of attention was also found to modulate P100 amplitude over lateral occipital sites, with significantly greater amplitude evoked by stimuli in attended locations. Regarding the present study, it appears reasonable to infer that since all stimuli were blocked in location, and for the RT conditions subjects were required to respond as quickly as possible, the implicit or ‘default’ strategy used to perform the task was covert orienting to the side of stimulation while maintaining central fixation. The relevance of the Mangun and Buck [49] data is that they demonstrate that covert orienting in this task facilitates response generation both behaviorally and physiologically. Therefore, it would be

expected for the RT conditions that electrocortical responses in the present study also reflect processes mediating sustained spatial attention, in addition to transient visuomotor activation.

Support for the existence of priming effects due to brief hemiretinal input comes from a recent study by Kim et al. [42]. These authors presented LVF or RVF primes 100–200 ms prior to presentation of a target stimulus in a Posner-type task [58]. The priming stimulus was a brief increase in the intensity of a square in which a target 'X' appeared with 50% probability. Thus, primes did not provide any net information on where the target would appear. Nonetheless, reaction times were delayed for invalidly cued targets, a finding similar to that obtained in this study in a task condition that used an arrow at central fixation to accurately predicted target location on 80% of trials. The brain regions activated during this task were then investigated in the same subjects using fMRI. Significant cortical activations were found bilaterally in FEF, banks of the intraparietal sulcus (IPS), SMA/anterior cingulate cortex, and left sensorimotor cortex. There was a marked asymmetry in IPS activation on the spatial priming task, such that right IPS showed a larger extent and intensity of activation than left IPS, even though responses were combined across the two visual fields. There was also a greater anterior spread of right compared with left frontal activation, which included right dorsolateral prefrontal cortex (posteriorly Brodmann's area (BA) 4, dorsally BA 9, and ventrally BA 44). These frontal data are consistent with the present findings, and provide functional evidence for preferential activation of right frontal regions during spatial attention tasks. Additional evidence for preferential involvement of right dorsolateral prefrontal cortex in tasks requiring spatial attention comes from a meta-analysis of neuroimaging studies investigating working memory [19]. Spatial attention tasks can be considered to include components of working memory since the effects are observed with SOAs on the order of 1 s (e.g. 100–800 ms [42]). Spatial working memory tasks resulted in greater right prefrontal activation than did non-spatial tasks [19]. Furthermore, in another study, right, but not left, dorsolateral prefrontal activations were observed by conjunction analysis of spatial and non-spatial attention using PET, and right anterior frontal activation was observed for both centrally presented and spatially distributed working memory tasks [16]. Since conjunction analysis identifies regions of common activation between tasks after subtraction of baseline conditions [59], these findings implicate right frontal involvement in multiple aspects of task performance including central fixation, peripheral attention, and action execution. Consistent with this claim, dorsolateral prefrontal activations have been observed in non-working memory tasks involving simple detection of a perifoveal cue during central fixation [20].

In addition to a role in spatial attention, frontal lobe functions of response inhibition may come into play in the present task situation in two principal ways: (1) inhibition of reflexive saccades to the hemiretinal stimuli; and (2) inhibition of overt motor responses during passive view trials. Prefrontal involvement in the inhibition of reflexive saccades comes from studies that show that lesions of dorsolateral prefrontal cortex increase the likelihood of pro-saccades during anti-saccade tasks [57,26,75,24]. Recently, single pulse transcranial magnetic stimulation (TMS) over right PFC has been applied coincident with peripheral visual stimuli in a saccadic gap paradigm [50]. TMS was shown to decrease saccade latency, interpreted as demonstrating the disinhibition of the oculomotor system by transient inactivation of PFC. Taken together, these data suggest that transient PFC activation might be expected during central fixation, with responses time-locked to visual input possibly reflecting contributions from active inhibition of execution of saccades programmed by the occurrence of peripheral visual input.

Regarding manual response inhibition, passive view trial blocks occurred interleaved with the RT task and self-initiated movement tasks (in a 1:5 ratio). Therefore, suppression of habitual RT responses was likely required to comply with the no-response task over the set of experimental sessions that contained 6000–7500 manual responses per subject. Recently, Konishi et al. [43] demonstrated preferential right compared with left inferior prefrontal activation during no-go trials using event-related fMRI. Subjects had to press left or right thumb buttons in response to centrally presented green, but not red, squares. Thus, active inhibition of motor output may also contribute to the pattern of right frontal activity observed in the present experiment.

It could be argued that the large degree of repetition of the visuomotor task in this experiment could modify responses during passive viewing trials such that memory of the motor response could account for the similarity in responses between passive and RT conditions. Yet the striking similarity of right frontocentral foci associated with left and right hand responses shown in Fig. 5 demonstrates that this activation is not movement-related since a manipulation as large as changing response hand does not change the pattern of frontal activation. However, movement-related responses are visible in this figure more centrally, and show marked differences both between left and right hand responses, and between RT and passive view conditions. Further, if motor imagery significantly contributed to the observed passive view response patterns, the temporal variability inherent in visualization would be expected to decrease the amplitude, and increase the peak latencies, of stimulus-triggered averages, which was not observed.

One way in which the RT motor task could have influenced the lateralization observed in the passive viewing condition is by way of creating a predominantly 'spatial' attentional set, both for visual input and motor output. The blocked design, and lack of motor selection,

may allow allocation of more resources to spatial processing and thus favor right hemisphere activations. The application of the present findings to more complex visuomotor tasks involving motor selection and stimulus–response associations, or their possible carry-over effects on embedded passive viewing trials, requires further study. Preferential left hemisphere involvement (in right handers) has been found with these task requirements (e.g., [67]), and thus the lateralization of frontal activations in more complex visuomotor tasks may differ from those of the simple blocked RT task presented here.

5. Summary and conclusion

In summary, the present study demonstrated electrocortical activations recorded over frontal cortex in response to hemiretinal stimuli that were separable from the time course of occipital activity, and that occurred independent of input visual field and motor response requirement. These activations were asymmetrical in that right frontal activity was more consistently observed than left frontal activations. The comparison of SCD and scalp potential data demonstrated the greater spatial resolution of SCD when used with high-density recordings. The presentation of individual subject data demonstrated the similarity of the main finding across subjects. The results suggest that frontal activation in response to hemiretinal visual input is consistent with a variety of cognitive and sensorimotor aspects of task performance that implicate frontal lobe function. These include allocation of spatial attention, maintenance of central fixation, and inhibition of motor responses during passive view trials. Such an interpretation would then suggest that the sensory-related activations in frontal and motor regions observed in the present study, even during ‘passive’ viewing, should not be considered as reflecting simply distributed visual efference, but rather as activations of multiple cortical regions involved in action intention as required by visuomotor tasks.

Acknowledgements

Sincere appreciation to Beth Higgins for help with data collection and manuscript preparation, and to Dr. J. Hrabe for software support. This work was supported by grants from NICHD (HD001799), NIMH (MH15788, MH11431, and MH60358) and NINDS (NS027900).

References

[1] G.K. Aguirre, E. Zarahn, M. D’esposito, The variability of human, BOLD hemodynamic responses, Neuroimage 8 (1998) 360–369.
[2] S.P. Ahlfors, R.J. Ilmoniemi, M.S. Hamalainen, Estimates of visually evoked cortical currents, Electroencephalogr. Clin. Neurophys. 82 (1992) 225–236.
[3] T.J. Anderson, I.H. Jenkins, D.J. Brooks, M.B. Hawken, R.S. Frackowiak, C. Kennard, Cortical control of saccades and fixation in man. A PET study, Brain 117 (1994) 1073–1084.
[4] L. Anllo-Vento, S.J. Luck, S.A. Hillyard, Spatio-temporal dynamics of attention to color: evidence from human electrophysiology, Hum. Brain Mapp. 6 (1998) 216–238.
[5] C. Asanuma, R.A. Andersen, W.M. Cowan, The thalamic relations of the caudal inferior parietal lobule and the lateral prefrontal cortex in monkeys: divergent cortical projections from cell clusters in the medial pulvinar nucleus, J. Comp. Neurol. 241 (1985) 357–381.
[6] F. Babiloni, C. Babiloni, L. Fattorini, F. Carducci, P. Onorati, A. Urbano, Performances of surface Laplacian estimators: a study of simulated and real scalp potential distributions, Brain Topogr. 8 (1995) 35–45.
[7] O. Blanke, S. Morand, G. Thut, C.M. Michel, L. Spinelli, T. Landis, M. Seeck, Visual activity in the human frontal eye field, Neuroreport 10 (1999) 925–930.
[8] L.D. Blumhardt, A.M. Halliday, Hemisphere contributions to the composition of the pattern-evoked potential waveform, Exp. Brain Res. 36 (1979) 53–69.
[9] G. Bonmassar, K. Anami, J. Ives, J.W. Belliveau, Visual evoked potential (VEP) measured by simultaneous 64-channel EEG and 3T fMRI, Neuroreport 10 (1999) 1893–1897.
[10] D. Boussaoud, S.P. Wise, Primate frontal cortex: effects of stimulus and movement, Exp. Brain Res. 95 (1993) 28–40.
[11] G.S. Brindley, The variability of the human striate cortex, J. Physiol. 225 (1972) 1–3.
[12] C. Cavada, P.S. Goldman-Rakic, Posterior parietal cortex in rhesus monkey: II. Evidence for segregated corticocortical networks linking sensory and limbic areas with the frontal lobe, J. Comp. Neurol. 287 (1989) 422–445.
[13] J.M. Clarke, E. Halgren, J.M. Scarabin, P. Chauvel, Auditory and visual sensory representations in human prefrontal cortex as revealed by stimulus-evoked spike-wave complexes, Brain 118 (1995) 473–484.
[14] M. Corbetta, E. Akbudak, T.E. Conturo, A.Z. Snyder, J.M. Ollinger, H.A. Drury, M.R. Linenweber, S.E. Petersen, M.E. Raichle, D.C. Van Essen, G.L. Shulman, A common network of functional areas for attention and eye movements, Neuron 21 (1998) 761–773.
[15] M. Corbetta, G.L. Shulman, Human cortical mechanisms of visual attention during orienting and search, Philos. Trans. Roy. Soc. Lond. B Biol. Sci. 353 (1998) 1353–1362.
[16] J.T. Coull, C.D. Frith, Differential activation of right superior parietal cortex and intraparietal sulcus by spatial and nonspatial attention, Neuroimage 8 (1998) 176–187.
[17] J.C. Culham, S.A. Brandt, P. Cavanagh, N.G. Kanwisher, A.M. Dale, R.B. Tootell, Cortical fMRI activation produced by attentive tracking of moving targets, J. Neurophysiol. 80 (1998) 2657–2670.
[18] C. Dao-fen, B. Hyland, V. Maier, A. Palmeri, M. Wiesendanger, Comparison of neural activity in the supplementary motor area and in the primary motor cortex in monkeys, Somatosens. Mot. Res. 8 (1991) 27–44.
[19] M. D’Esposito, G.K. Aguirre, E. Zarahn, D. Ballard, R.K. Shin, J. Lease, Functional MRI studies of spatial and nonspatial working memory, Cognit. Brain Res. 7 (1998) 1–13.
[20] M. D’Esposito, D. Ballard, G.K. Aguirre, E. Zarahn, Human prefrontal cortex is not specific for working memory: a functional MRI study, Neuroimage 8 (1998) 274–282.
[21] E.A. DeYoe, G.J. Carman, P. Bandettini, S. Glickman, J. Wieser, R. Cox, D. Miller, J. Neitz, Mapping striate and extrastriate visual areas in human cerebral cortex, Proc. Natl. Acad. Sci. USA 93 (1996) 2382–2386.
[22] H.E. Egeth, S. Yantis, Visual attention: control, representation, and time course, Annu. Rev. Psychol. 48 (1997) 269–297.
[23] H. Endo, T. Kizuka, T. Masuda, T. Takeda, H. T, Endo, Automatic

activation in the human primary motor cortex synchronized with movement preparation, Cognit. Brain Res. 8 (1999) 229–239.
[24] S. Everling, B. Fischer, The antisaccade: a review of basic research and clinical studies, Neuropsychologia 36 (1998) 885–899.
[25] V.P. Ferrera, J.K. Cohen, B.B. Lee, Activity of prefrontal neurons during location and color delayed matching tasks, Neuroreport 10 (1999) 1315–1322.
[26] J. Fukushima, K. Fukushima, K. Miyasaka, I. Yamashita, Voluntary control of saccadic eye movement in patients with frontal cortical lesions and Parkinsonian patients in comparison with that in schizophrenics, Biol. Psychiatry 36 (1994) 21–30.
[27] S. Funahashi, C.J. Bruce, P.S. Goldman-Rakic, Visuospatial coding in primate prefrontal neurons revealed by oculomotor paradigms, J. Neurophysiol. 63 (1990) 814–831.
[28] S. Funahashi, M.V. Chafee, P.S. Goldman-Rakic, Prefrontal neuronal activity in rhesus monkeys performing a delayed anti-saccade task, Nature 365 (1993) 753–756.
[29] L.F. Garey, B. Dreher, S.R. Robinson, The organization of the visual thalamus, in: B. Dreher, S.R. Robinson (Eds.), J.R. Cronly-Dillon (Series Ed.), Vision and Visual Dysfunction, Vol. 3: Neuroanatomy of the Visual Pathways and Their Development. CRC Press Inc, Boca Raton, 1991, pp. 176–234.
[30] M.S. Graziano, X.T. Hu, C.G. Gross, Visuospatial properties of ventral premotor cortex, J. Neurophysiol. 77 (1997) 2268–2292.
[31] R. Hajdukovic, B.A. Allen, R.G. Bickford, Frontal processing of PVEPs as indicated by contour studies, Electroencephalogr. Clin. Neurophys. 58 (1984) 13P.
[32] A.M. Halliday, G. Barrett, L.D. Blumhardt, A. Kriss, The macular and paramacular subcomponents of the pattern evoked response, in: D. Lehmann, E. Callaway (Eds.), Human Evoked Potentials: Applications and Problems, Plenum, New York, 1979, pp. 135–151.
[33] T. Hashimoto, S. Kashii, M. Kikuchi, Y. Honda, T. Nagamine, H. Shibasaki, Temporal profile of visual evoked responses to pattern-reversal stimulation analyzed with a whole-head magnetometer, Exp. Brain Res. 125 (1999) 375–382.
[34] M.K. Hasnain, P.T. Fox, M.G. Woldorff, Intersubject variability of functional areas in the human visual cortex, Hum. Brain Mapp 6 (1998) 301–315.
[35] J.R. Hughes, A. Kuruvilla, J.J. Fino, Topographic analysis of visual evoked potentials from flash and pattern reversal stimuli: evidence for 'travelling waves', Brain Topogr. 4 (1992) 215–228.
[36] H. Ikeda, H. Nishijo, K. Miyamoto, R. Tamura, S. Endo, T. Ono, Generators of visual evoked potentials investigated by dipole tracing in the human occipital cortex, Neuroscience 84 (1998) 723–739.
[37] S.I. Ito, Prefrontal unit activity of macaque monkeys during auditory and visual reaction time tasks, Brain Res. 247 (1982) 39–47.
[38] F. Karayanidis, P.T. Michie, Frontal processing negativity in a visual selective attention task, Electroencephalogr. Clin. Neurophys. 99 (1996) 38–56.
[39] S. Kastner, M.A. Pinsk, P. De Weerd, R. Desimone, L.G. Ungerleider, Increased activity in human visual cortex during directed attention in the absence of visual stimulation, Neuron 22 (1999) 751–761.
[40] H. Kawamichi, Y. Kikuchi, H. Endo, T. Takeda, S. Yoshizawa, Temporal structure of implicit motor imagery in visual hand–shape discrimination as revealed by MEG, Neuroreport 9 (1998) 1127–1132.
[41] D.N. Kennedy, N. Lange, N. Makris, J. Bates, J. Meyer, V.S. Caviness Jr., Gyri of the human neocortex: an MRI-based analysis of volume and variance, Cereb. Cortex 8 (1998) 372–384.
[42] Y.H. Kim, D.R. Gitelman, A.C. Nobre, T.B. Parrish, K.S. LaBar, M.M. Mesulam, The large-scale neural network for spatial attention displays multifunctional overlap but differential asymmetry, Neuroimage 9 (1999) 269–277.
[43] S. Konishi, K. Nakajima, I. Uchida, H. Kikyo, M. Kameyama, Y. Miyashita, Common inhibitory mechanism in human inferior prefrontal cortex revealed by event-related functional MRI, Brain 122 (1999) 981–991.
[44] S. Kurita-Tashima, S. Tobimatsu, M. Kato, Frontal negativity of pattern-reversal visual evoked potentials in humans, Neurosci. Res. 10 (1991) 52–63.
[45] S. Kurita-Tashima, S. Tobimatsu, M. Nakayama-Hiromatsu, M. Kato, The neurophysiologic significance of frontal negativity in pattern-reversal visual-evoked potentials, Invest. Ophthalmol Vis. Sci. 33 (1992) 2423–2428.
[46] G. Luppino, M. Matelli, R. Camarda, G. Rizzolatti, Corticocortical connections of area F3 (SMA-proper) and area F6 (pre-SMA) in the macaque monkey, J. Comp. Neurol. 338 (1993) 114–140.
[47] B. Luna, K.R. Thulborn, M.H. Strojwas, B.J. McCurtain, R.A. Berman, C.R. Genovese, J.A. Sweeney, Dorsal cortical regions subserving visually guided saccades in humans: an fMRI study, Cereb. Cortex 8 (1998) 40–47.
[48] J. Maier, G. Dagnelie, H. Spekreijse, B.W. van Dijk, Principal components analysis for source localization of VEPs in man, Vision Res. 27 (1987) 165–177.
[49] G.R. Mangun, L.A. Buck, Sustained visual–spatial attention produces costs and benefits in response time and evoked neural activity, Neuropsychologia 36 (1998) 189–200.
[50] R.M. Muri, S. Rivaud, B. Gaymard, C.J. Ploner, A.I. Vermersch, C.W. Hess, C. Pierrot-Deseilligny, Role of the prefrontal cortex in the control of express saccades: A transcranial magnetic stimulation study, Neuropsychologia 37 (1999) 199–206.
[51] M.S. Myslobodsky, R. Coppola, D.R. Weinberger, EEG laterality in the era of structural brain imaging, Brain Topography 3 (1991) 381–390.
[52] R.C. Oldfield, The assessment and analysis of handedness: the Edinburgh inventory, Neuropsychologia 9 (1971) 97–113.
[53] P. Ossenblok, H. Spekreijse, The extrastriate generators of the EP to checkerboard onset, A source localization approach, Electroencephalogr. Clin. Neurophys. 80 (1991) 181–193.
[54] F. Perrin, O. Bertrand, J. Pernier J, Scalp current density mapping: value and estimation from potential data, IEEE Trans. Biomed. Eng. 34 (1987) 283–288.
[55] F. Perrin, J. Pernier, O. Bertrand, J.F. Echallier, Spherical splines for scalp potential and current density mapping, Electroencephalogr. Clin. Neurophys. 72 (1989) 184–187.
[56] M. Petrides, D.N. Pandya, Dorsolateral prefrontal cortex: comparative cytoarchitectonic analysis in the human and the macaque brain and corticocortical connection patterns, Eur. J. Neurosci. 11 (1999) 1011–1036.
[57] C. Pierrot-Deseilligny, S. Rivaud, B. Gaymard, Y. Agid, Cortical control of reflexive visually-guided saccades, Brain 114 (1991) 1473–1485.
[58] M.I. Posner, Orienting of attention, Q.J. Exp. Psychol. 32 (1980) 3–25.
[59] C.J. Price, K.J. Friston, Cognitive conjunction: a new approach to brain activation experiments, Neuroimage 5 (1997) 261–270.
[60] A. Riehle, Visually induced signal-locked neuronal activity changes in precentral motor areas of the monkey: hierarchical progression of signal processing, Brain Res. 540 (1991) 131–137.
[61] A. Riehle, J. Requin, Monkey primary motor and premotor cortex: single-cell activity related to prior information about direction and extent of an intended movement, J. Neurophysiol. 61 (1989) 534–549.
[62] G. Rizzolatti, G. Luppino, M. Matelli, The organization of the cortical motor system: new concepts, Electroencephalogr. Clin. Neurophys. 106 (1998) 283–296.
[63] T. Ro, S. Cheifet, H. Ingle, R. Shoup, R. Rafal, Localization of the human frontal eye fields and motor hand area with transcranial magnetic stimulation and magnetic resonance imaging, Neuropsychologia 37 (1999) 225–231.
[64] J.D. Schall, Neuronal activity related to visually guided saccadic eye movements in the supplementary motor area of rhesus monkeys, J. Neurophysiol. 66 (1991) 530–558.
[65] J.D. Schall, Visuomotor areas of the frontal lobe, in: K.S. Rockland,

J.H. Kaas, A. Peters (Eds.), E.G. Jones, A. Peters (Series Eds.), Cerebral Cortex, Vol. 12, Extrastriate Cortex in Primates, Plenum, New York, 1997, pp. 527–638.

[66] J.D. Schall, D.P. Hanes, K.G. Thompson, D.J. King, Saccade target selection in frontal eye field of macaque: I. Visual and premovement activation, J. Neurosci. 15 (1995) 6905–6918.

[67] N.D. Schulter, M.F.S. Rushworth, R.E. Passingham, K.R. Mills, Temporary interference in human lateral premotor cortex suggests dominance for the selection of movements: a study using transcranial magnetic stimulation, Brain 121 (1998) 785–799.

[68] G.V. Simpson, J.J. Foxe, H.G. Vaughan Jr., A.D. Mehta, C.E. Schroeder, Integration of electrophysiological source analyses, MRI and animal models in the study of visual processing and attention, Electroencephalogr. Clin. Neurophys. Suppl. 44 (1995) 76–92.

[69] G.V. Simpson, M.E. Pflieger, J.J. Foxe, S.P. Ahlfors, H.G. Vaughan Jr., J. Hrabe, R.J. Ilmoniemi, G. Lantos, Dynamic neuroimaging of brain function, J. Clin. Neurophys. 12 (1995) 432–449.

[70] R. Srebro, The topography of scalp potentials evoked by pattern pulse stimuli, Vision Res. 27 (1987) 901–914.

[71] S.S. Stensaas, D.K. Eddington, W.H. Dobelle, The topography and variability of the primary visual cortex in man, J. Neurosurg. 40 (1974) 747–755.

[72] S. Thorpe, D. Fize, C. Marlot, Speed of processing in the human visual system, Nature 381 (1996) 520–522.

[73] G. Thut, C.A. Hauert, O. Blanke, S. Morand, M. Seeck, S.L. Gonzalez, R. Grave de Peralta, L. Spinelli, A. Khateb, T. Landis, C.M. Michel, Visually induced activity in human frontal motor areas during simple visuomotor performance, Neuroreport 11 (2000) 2843–2848.

[74] H.G. Vaughan Jr., Topographic analysis of brain electrical activity, Electroencephalogr. Clin. Neurophys. Suppl. 39 (1987) 137–142.

[75] R. Walker, M. Husain, T.L. Hodgson, J. Harrison, C. Kennard, Saccadic eye movement and working memory deficits following damage to human prefrontal cortex, Neuropsychologia 36 (1998) 1141–1159.

[76] S.P. Wise, D. Boussaoud, P.B. Johnson, R. Caminiti, Premotor and parietal cortex: corticocortical connectivity and combinatorial computations, Annu. Rev. Neurosci. 20 (1997) 25–42.

[77] J. Zhang, A. Riehle, J. Requin, S. Kornblum, Dynamics of single neuron activity in monkey primary motor cortex related to sensorimotor transformation, J. Neurosci. 17 (1997) 2227–2246.